International Journal of Microwave and Wireless Technologies

cambridge.org/mrf

Research Paper

Cite this article: Cahyasiwi DA, Roza E, Mujirudin M, Nashuha NM, Zulkifli FY, Rahardjo ET (2022). Selectivity improvement of interdigital filtering-antenna using different orders for 5 G application. *International Journal of Microwave and Wireless Technologies* 1–9. https://doi.org/10.1017/S1759078722001143

Received: 19 June 2022
Revised: 22 September 2022
Accepted: 23 September 2022

Key words:
5G; filtering antenna; interdigital resonator; selectivity

Author for correspondence:
Dwi Astuti Cahyasiwi,
E-mail: dwi.cahyasiwi@uhamka.ac.id

Selectivity improvement of interdigital filtering-antenna using different orders for 5 G application

Dwi Astuti Cahyasiwi[1], Emilia Roza[1], Mohammad Mujirudin[1], Nusriyati Mahmuda Nashuha[1], Fitri Yuli Zulkifli[2] and Eko Tjipto Rahardjo[2]

[1]Department of Electrical Engineering, Universitas Muhammadiyah Prof. DR. HAMKA, Jl. Tanah Merdeka, Jakarta Timur, Indonesia and [2]Department of Electrical Engineering, Universitas Indonesia, Depok, Indonesia

Abstract

In this paper, filter and antenna integration is studied to produce a compact device for wireless front-end equipment. Filtering antennas are advanced due to their selectivity performance, represented by a flat gain response. Two filtering antennas are proposed to improve the selectivity using different orders. The first antenna is based on second-order filter and the other on third-order filter. Both antennas are designed to operate at 4.65 GHz for mid-band 5 G application with a bandwidth of 6.45%. The first antenna integrates a rectangular radiator and an interdigital resonator based on second-order filter. It obtained a bandwidth impedance of −10 dB for 300 MHz and a maximum gain of 6.48 dBi. Meanwhile, the second design consists of a rectangular radiator and two interdigital resonators based on third-order filter as the feedline. Having the same bandwidth as the first design, the second design achieved a flat gain of 6.37 dBi in the operational bandwidth. The second antenna design showed better selectivity with sharper gain than the first design. The two antennas were fabricated and measured for validation. The simulation and measurement results showed good agreement.

Introduction

Future wireless telecommunication equipment requires multifunctional, integrated, and compact devices. Antennas and filters are circuits at the wireless front end that were traditionally parted. However, nowadays, the integration of the two circuits what is known as a filtering antenna is widely researched [1–5]. A filtering antenna adds a radiator with a selectivity feature, which is represented by a flat gain within the operational bandwidth and two radiation nulls at the upper and lower frequencies. Moreover, this antenna results in the integration of an antenna and a filter without insertion loss and with more compact features.

The most common method of designing a filtering antenna involves replacing the last filter stage with a radiator [6–9]. In addition, some resonators have been used to design filtering antennas, e.g. hairpins [10, 11], stub resonators [8, 12], U-resonators [13, 14], ring resonators [15], and interdigital resonators [3, 16]. The co-design of an antenna and a filter able to produce a miniaturized front-end device with selectivity is based on the filter design. In other words, the order of the filter used affects the filter selectivity, which applies to the filtering antenna based on the co-design. Reference [17] compares filtering antennas of different orders using simulation method; a square-ring resonator was used, but the study has no measurement validation results. The F and L inverted filtering antennas, based on the third- and fourth-order filters, respectively, are synthesized in [18]; however, both antennas use different resonators, and no comparison between the two orders has been conducted.

Reference [3] used two interdigital resonators to design two filtering antennas with vertical and 45° polarization features; however, no measurement result was presented for the antenna with vertical polarization based on the third-order filter. Although a measurement for this type of filtering antenna was offered by [16], the design was not based on the second-order filter because the radiator extraction size was sufficiently wide to obtain slant polarization. The antenna based on a second-order filter has less selectivity than that based on a third-order filter, and no extraction is performed.

In the co-design of a filtering antenna, radiator extraction is essential because, with various radiator sizes, we can generate the same frequency operation but with different radiation values. Furthermore, the radiation quality (Q_{rad}) significantly affects the operating bandwidth produced by the filtering antenna, which must have the same value as the external quality of the filter in the co-design.

In this study, we propose two configurations of the filtering antennas using the interdigital resonator based on second- and third-order filters to improve the selectivity. Both designs use

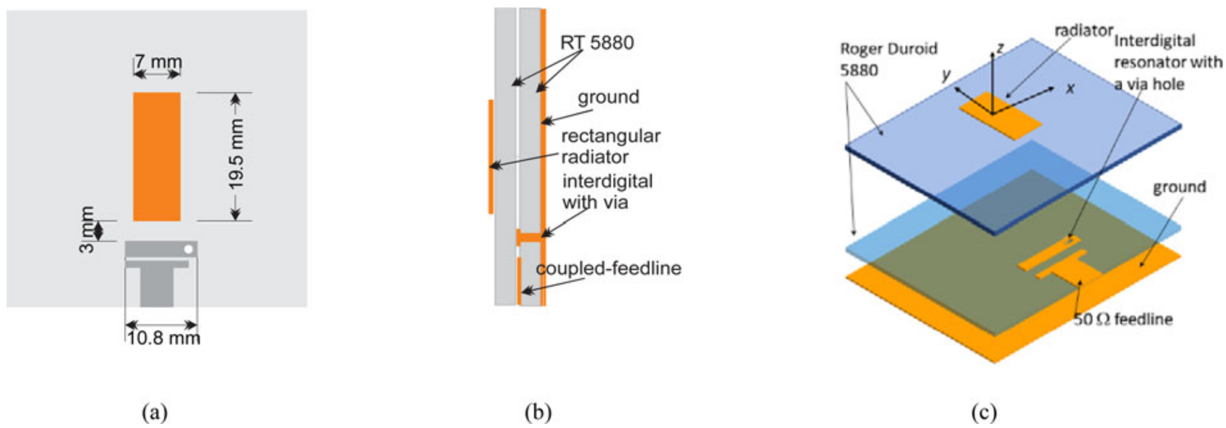

Fig. 1. (a) Geometric structure, (b) side view, and (c) perspective view of Ant. I.

a rectangular radiator, and they are integrated to obtain an operational frequency of 4.65 GHz with a bandwidth of 6.45% for 5 G application. The antenna is proximity fed, with all structures couple connected. The measurement results validate the designs and are consistent with the simulations. It is proven that using a higher order, the third-order selectivity is better than the second-order.

Design and method

In this paper, we discuss filter antennas of different orders. The first design, Ant. I, is a filtering antenna based on second-order filters, while the second design, i.e. Ant. II, is based on third-order filter extraction. The geometric structure of Ant. I can be seen in Fig. 1(a), where it consists of two layers of substrates, a 7 mm × 19.5 mm rectangular radiator is on the first layer, and there is a feeding circuit that comprises an interdigital resonator coupled with a 50 ohm transmission line on the second layer. Figure 1(b) shows the design from the side view, and Fig. 1(c) is the exploded view of the two layers. Figure 2(a) shows the geometric structure of Ant. II, which consists of a 2.1 mm × 19.5 mm radiator on the top substrate that is proximity-coupled with the feeding network on the second substrate. Two interdigital resonators coupled with a 50 ohm transmission line are on the second substrate. A through hole with a diameter of 1.2 mm is set alternately at each end of the resonator's arm. There is 3.4 mm of space between the radiator and resonator and 5.9 mm of space between the two alternate resonators. The 50 ohm transmission line is coupled with a 0.7 mm gap. All structures are printed on two layers of 50 mm × 50 mm substrates. Figure 2(b) shows the antenna from the side view, which consists of a rectangular radiator on the top substrate and a feeding circuit at the bottom, while Fig. 2(c) shows the exploded view of the design. Both Ant. I and Ant. II use an interdigital resonator sized 2.4 mm × 10.8 mm and a through hole with a diameter of 1.2 mm.

The two designs are based on second- and third-order extraction filters, and both antennas are designed to operate at a frequency of 4.65 GHz and an operating bandwidth of 300 MHz or 6.45%. Following [19], all lowpass filter parameters with a ripple of 0.2 dB are presented in Table 1. Furthermore, using (1) and (2) outlined in [20], the coupling parameters, radiation quality (Q_{rad}), and external quality (Q_{ext}) can be calculated where FBW

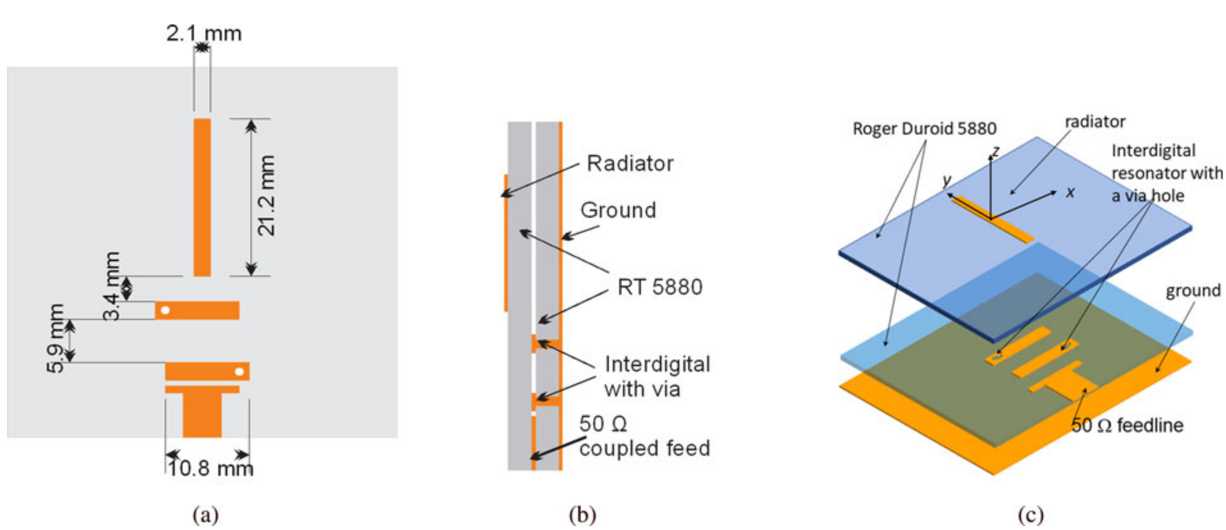

Fig. 2. (a) Geometric structure, (b) side view, and (c) perspective view of Ant. II.

https://doi.org/10.1017/S1759078722001143 Published online by Cambridge University Press

Table 1. Parameter filter extraction for second- and third-order filters

Parameter	Second-order	Third-order
Ripple (dB)	0.2	0.2
g_0	1	1
g_1	0.843	1.2276
g_2	0.622	1.1525
g_3	1.3554	1.2276
g_4		1
Frequency (GHz)	4.65	4.65
BW (GHz)	0.3	0.3
FBW	0.064516	0.064516129
Q_{ext}	13.0665	19.0278
Q_{rad}		19.0278
$K_{1,2}$	0.070268	0.054239964
$K_{3,4}$	–	0.054239964

is the fractional bandwidth, the results of which are shown in Table 1.

$$Q_{ext} = \frac{g_n g_{n+1}}{FBW}, \quad (1)$$

$$M_{i,i+1} = \frac{FBW}{\sqrt{g_i g_{i+1}}}. \quad (2)$$

Next, we extract the radiator and resonator using (3) and (4), and CST simulation tools where f_c is the center frequency, and $\triangle f$ is f_2–f_1. The structure extraction is conducted to obtain the resonant frequency and Q_{rad} each for Ant. I and Ant. II. The radiator extraction also proves that to obtain a 4.65 GHz resonance, we can use different-sized rectangular radiators, as in Ant. I and Ant. II. The length (L_p) and width (W_p) of the Ant. I radiator, shown in Fig. 3(a), are 19.96 and 8.25 mm, respectively, to generate a 4.65 GHz operational frequency and Q_{rad} of 13.06. A Q_{rad} of 19.02 and operational frequency of 4.65 GHz can be obtained when the L_p and W_p of the Ant. II radiator are 21.2 and 2.8 mm, as shown in Fig. 3(b). Figure 4(a) shows the relation between W_p and Q_{rad} at an operating frequency of 4.65 GHz; to obtain higher Q_{rad} values, W_p should be reduced. The resonator's resonant frequency of 4.65 GHz is extracted by simulating the structure, as shown in Fig. 4(b).

$$Q_{rad} = \frac{f_c}{\triangle f}, \quad (3)$$

$$M_{n,n+1} = \frac{f_{n+1}^2 - f_n^2}{f_{n+1}^2 + f_n^2}. \quad (4)$$

The parametric study shows that the interdigital resonates at 4.65 GHz with a length (P_k) of 10.8 mm. The shorter the P_k the higher is the frequency resonance. For Ant. II, based on third-order filter extraction, it is necessary to ensure coupling between two resonators. A coupling value of 0.0542 is obtained using the two-port extraction curve from [3] when the distance between the two resonators (Gap_1) is approximately 5.1 mm, as shown in Fig. 5(a). The coupling between the resonator and radiator is depicted in Fig. 5(b), with Q_{rad} values of 13 and 19 for Ant. I and Ant. II, respectively. This shows that the distance between the resonator and radiator (C_B) to obtain the associated coupling values (0.0702 and 0.0542) is around 3.87 mm for Ant. I and 3.65 mm for Ant. II. Finally, the initial dimensions of the two designs are achieved from these extractions.

Results and discussion

From the S_{11} response of Ant. I in the initial design of Fig. 6(a), it is evident that the red curve does not convey the character of a second-order filter due to its single minimum value, and neither the bandwidth nor the center frequency parameters meet the desired values. Moreover, the design optimization result on the black curve shows the S_{11} response, which is identical to a second-order filter response with two minimum values. As required, the center frequency occurs at 4.65 GHz, with an S_{11} of −12.1 and −10 dB bandwidth impedance in the 4.48–4.8 GHz range. Figure 6(b) shows the initial design of Ant. II, where the S_{11} response has three minimal values. However, the −10 dB bandwidth impedance is yet to be obtained. After optimization, as shown via the black curve, the −10 dB bandwidth

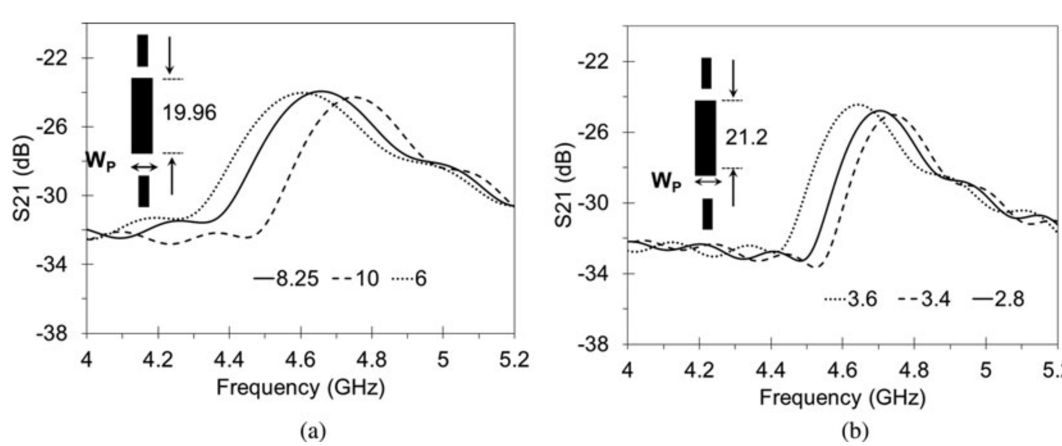

Fig. 3. The Q_{rad} simulation extraction structure under different W_p values of (a) Ant. I and (b) Ant. II (all unit dimensions in mm).

https://doi.org/10.1017/S1759078722001143 Published online by Cambridge University Press

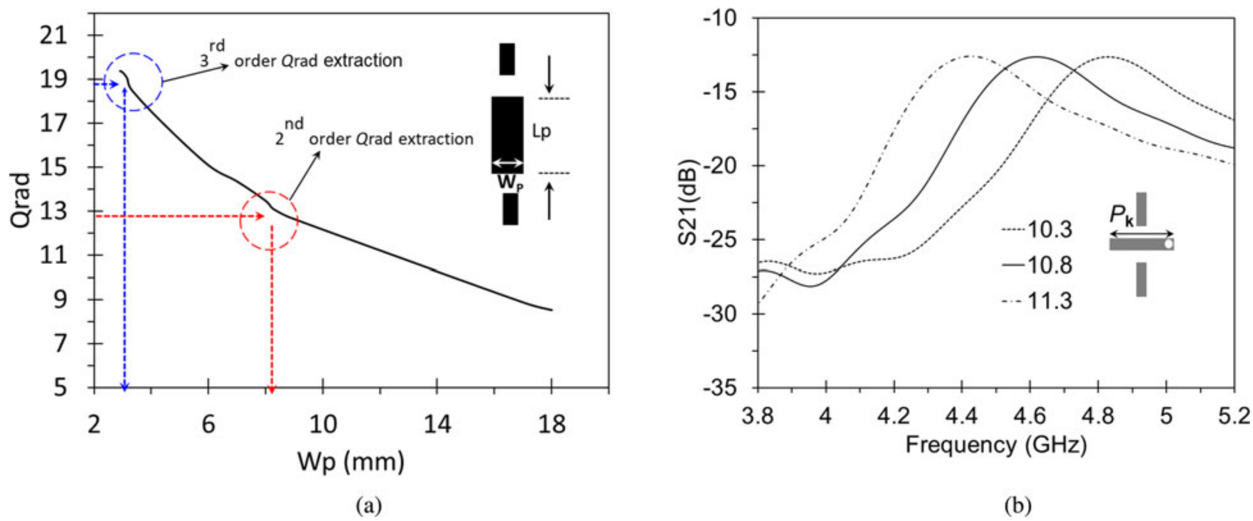

Fig. 4. (a) The Q_{rad} values of Ant. I (red arrow) and Ant. II (blue arrow), (b) the interdigital resonator's resonance at different lengths (P_k) with a thickness of 2.4 mm.

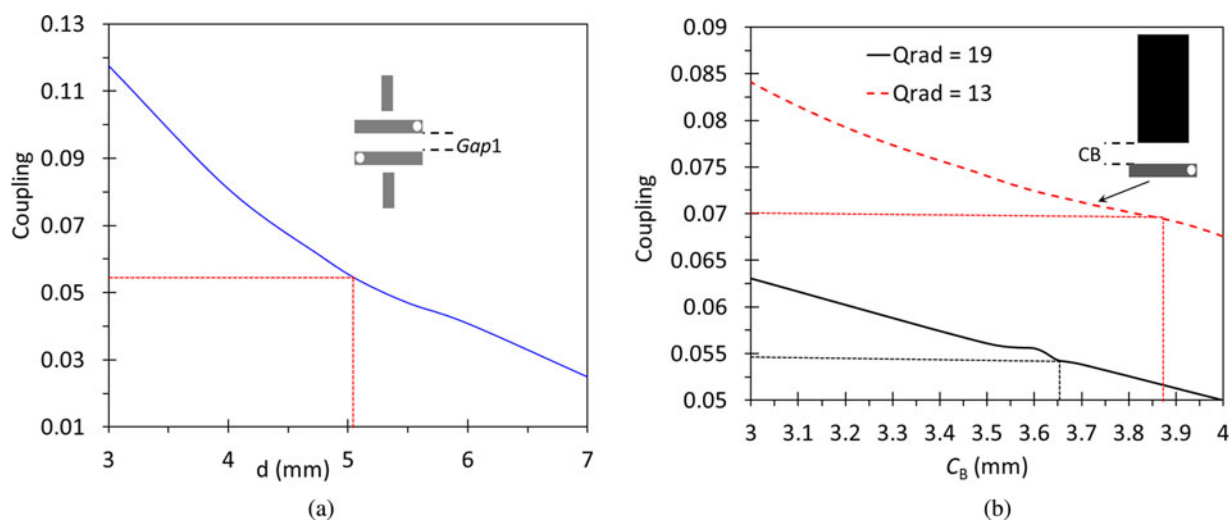

Fig. 5. (a) Coupling structure between two resonators for Ant. II and (b) the coupling between the radiator and resonator of Ant. I ($Q_{rad} = 19$) and Ant. II ($Q_{\mathrm{rad}} = 13$) under different C_B values.

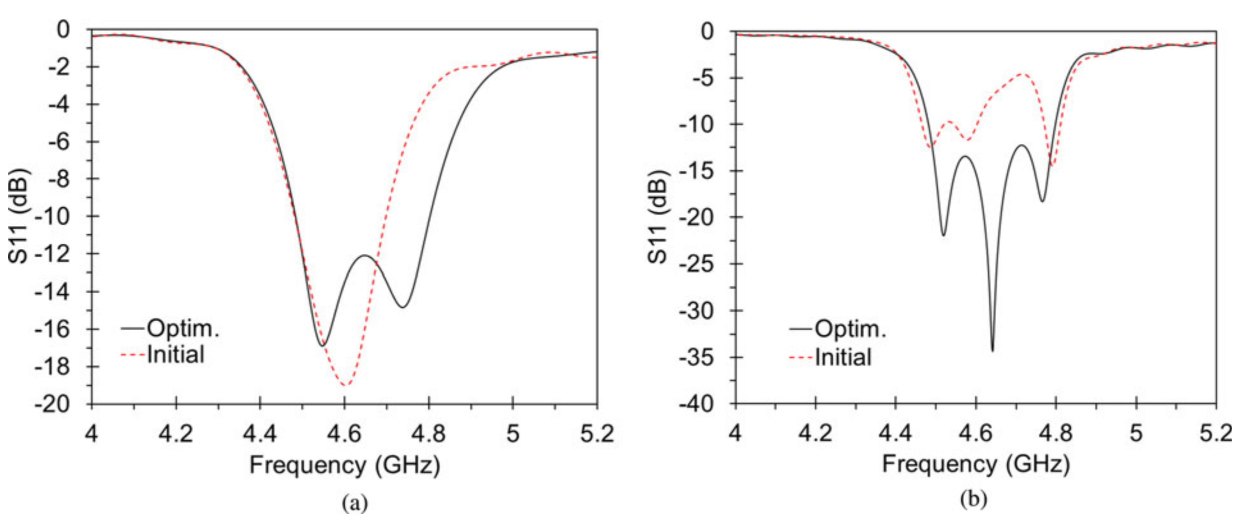

Fig. 6. (a) The initial and optimized designs of second-order and (b) third-order interdigital filtering antennas.

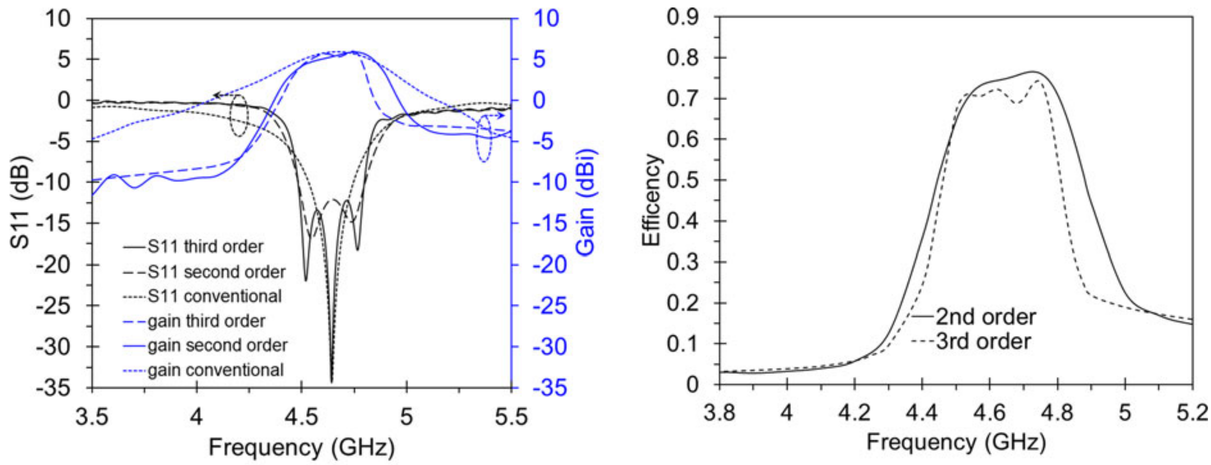

(a) (b)

Fig. 7. (a) The optimized S_{11} and gain simulation comparison of the second- and third-order and (b) the efficiency of the second- and third-order interdigital filtering antennas.

impedance for a frequency range of 4.482–4.798 GHz is achieved with a center frequency of 4.65 GHz and a minimum S_{11} value of −34 dB.

Figure 7(a) compares the S_{11} values and gain responses of the two designs with conventional antennas without an integrated filter. Ant. I with an S_{11} response as a second-order filter has a maximum gain of 5.89 dBi at 4.75 GHz, and the gain hovers around 5 dBi up to a frequency of 4.825 GHz, still high outside the operating bandwidth. Meanwhile, Ant. II has a maximum gain of 5.92 at 4.75 GHz and drops sharply to 1 dBi at 4.85 GHz. This shows that Ant. II blocks power beyond its operating bandwidth (4.5–4.8 GHz range) better than Ant. I. However, the selectivity of Ant. I is better than the conventional antenna because a traditional antenna's gain response decreases with a slope, so it does not resemble the response of a bandpass filter. In addition, the proposed designs have a wider bandwidth (300 MHz) than a conventional antenna (214 MHz). A comparison of both filtering antennas' efficiencies is shown in Fig. 7(b), where Ant. II has more ripple and a sharper curve than Ant. I. The maximum efficiencies of Ant. I and Ant. II are 0.78 and 0.75, respectively. The decreased efficiency from Ant. I and Ant. II can be attributed to the radiator size of Ant. II that is narrower than Ant. I.

Both designs were fabricated and measured in an anechoic chamber for validation purposes. The fabricated filtering antennas are shown in Fig. 8, which depicts that Ant. I's radiator has a broader size compared to that of Ant. II. Using a ZNB 40 vector network analyzer, S_{11} and the gain response were measured. Figure 9(a) compares the S_{11} values obtained from the simulation and measurement results for Ant. I, from which it is evident that Ant. I has a −10 dB bandwidth impedance for a range of 4.501–4.847 GHz, which is 9% wider (and shifted to a higher frequency) compared to the simulation results. Figure 9(b) compares the S_{11} values obtained from Ant. II's simulation and measurement results, from which it is evident that the measurement results shift to a higher frequency and have a 10% wider bandwidth for a range of 4.506–4.839 GHz compared to the simulation results. Figure 10(a) shows the Ant. I's gain measurement results, which slightly shifted to the upper frequency compared to the simulation results. With a maximum value of 6.48 dBi at 4.8 GHz, the measurement result is 0.6 dB higher than the simulation. Figure 10(b) shows that Ant. II's maximum gain is 6.37 dBi at 4.8 GHz, which decreases sharply to −15 dBi at 4.89 GHz, which indicates a gain blocking of 21 dB in both the lower and upper frequencies. Similar to the S_{11} response, the gain response of both antennas also shifts toward higher frequencies. The discrepancy between the simulation and measurement results can be attributed to the two-layer design. In particular, a tiny air gap may exist between the layers, which explains the shift in operational frequency; otherwise, the shift may be due to substrate permittivity tolerance and fabrication errors. The S_{11} simulation and measurement results of Ant. I in Fig. 11(a) show that with two minimal values, the parameter is characterized as a second-order filter, while Ant. II has three minimum values that correspond to the third-order filter response. The Ant. I and Ant. II selectivity comparison in Fig. 11(b) shows that Ant. II has a sharper bandpass filter response than Ant. I in the same operational bandwidth.

Figure 12 shows the normalized simulation and measurement radiation pattern of Ant. I at 4.65 GHz. The antenna has a

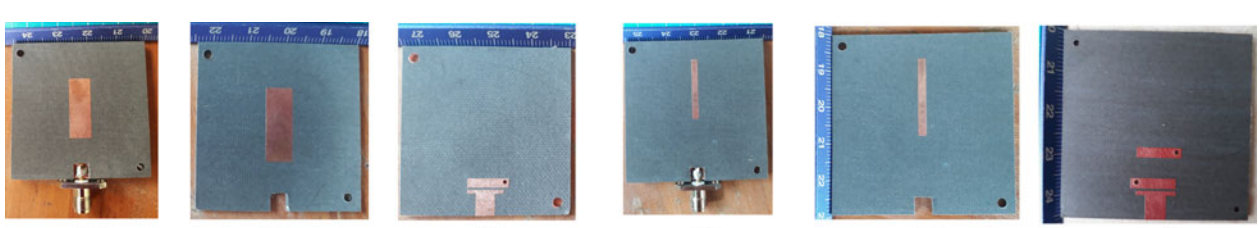

(a) (b) (c) (d) (e) (f)

Fig. 8. Fabrication (a) assembled (b) radiator on the first layer (c) filtering circuit of Ant. I, (d) assembled (e) radiator on the first layer (f) filtering circuit of Ant. II.

https://doi.org/10.1017/S1759078722001143 Published online by Cambridge University Press

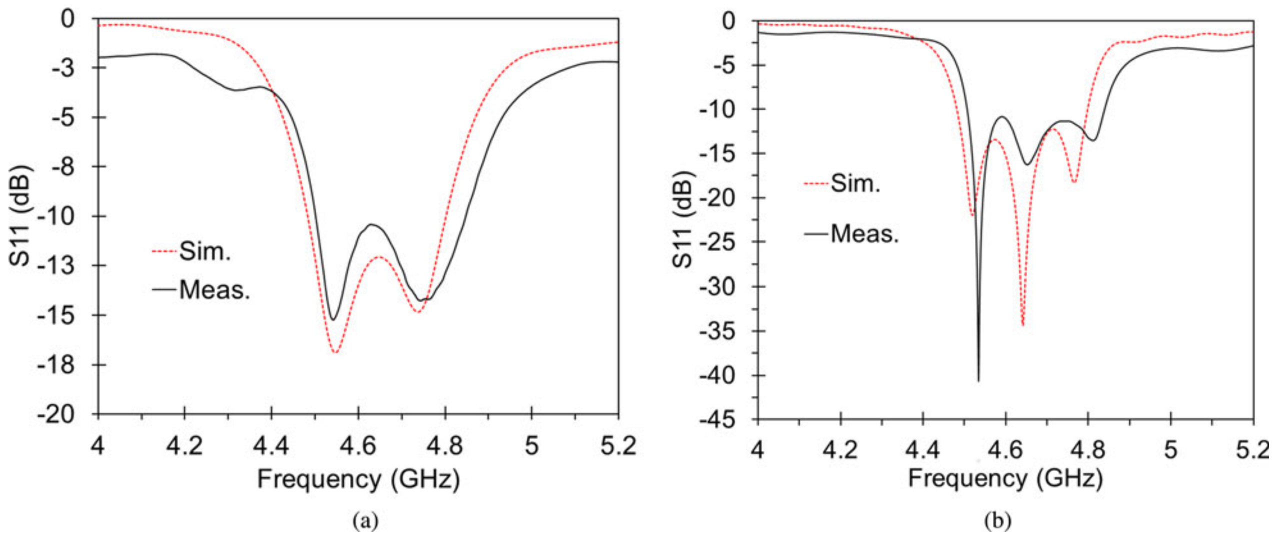

Fig. 9. The S_{11} measurement and simulation results comparison of (a) the second- and (b) third-order filtering antennas.

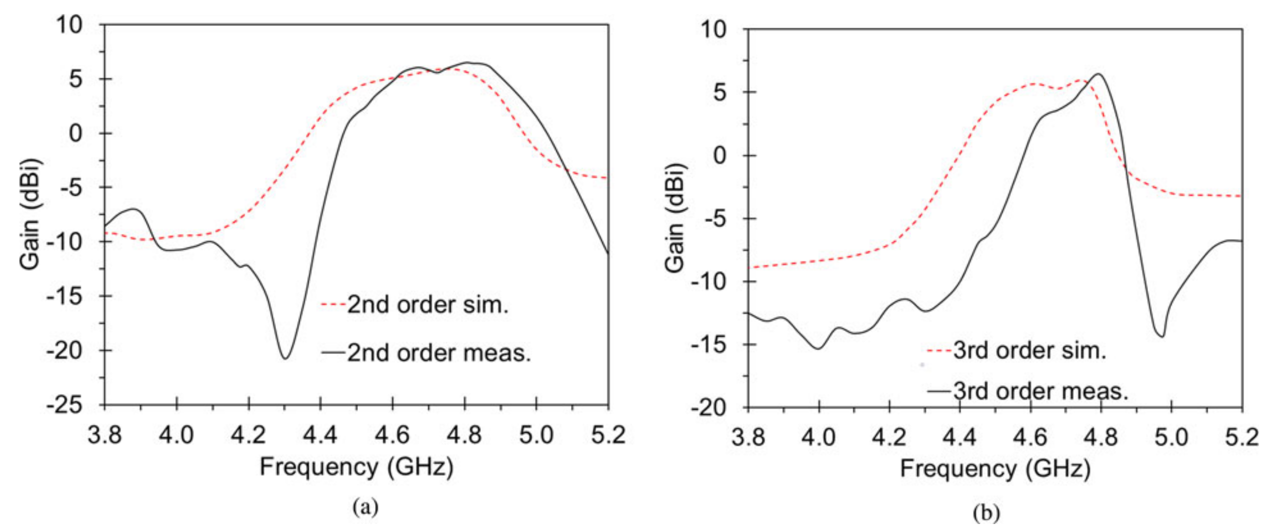

Fig. 10. (a) Ant. I's gain comparison of simulation and measurement results, (b) Ant. II's gain comparison of simulation and measurement results.

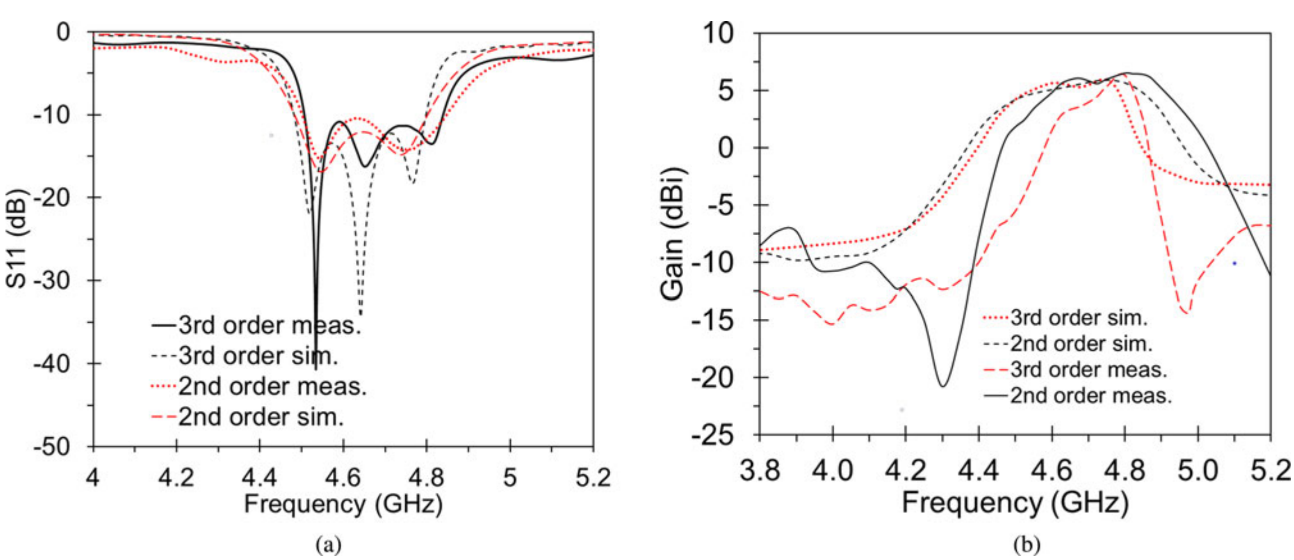

Fig. 11. (a) S_{11} measurement and simulation results comparison of the second- and third-order filtering antennas and (b) gain measurement and simulation results comparison of the second- and third-order filtering antennas.

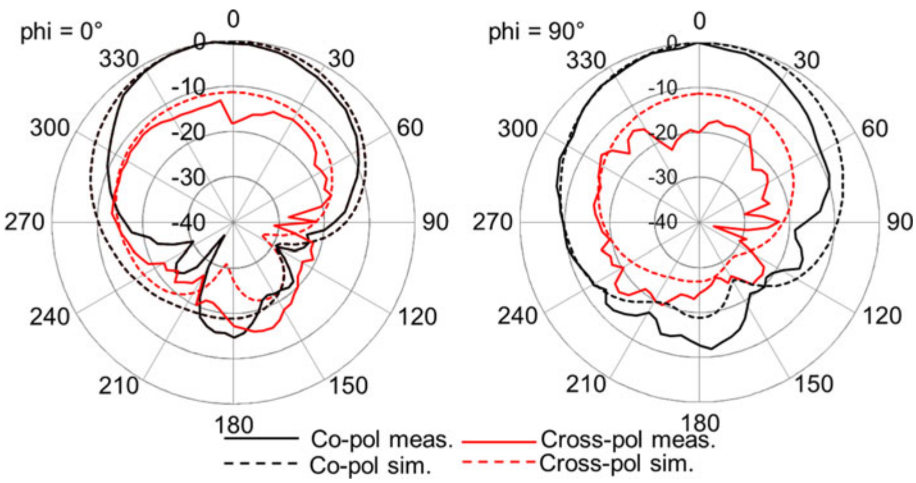

Fig. 12. Ant. I's radiation pattern at 4.65 GHz.

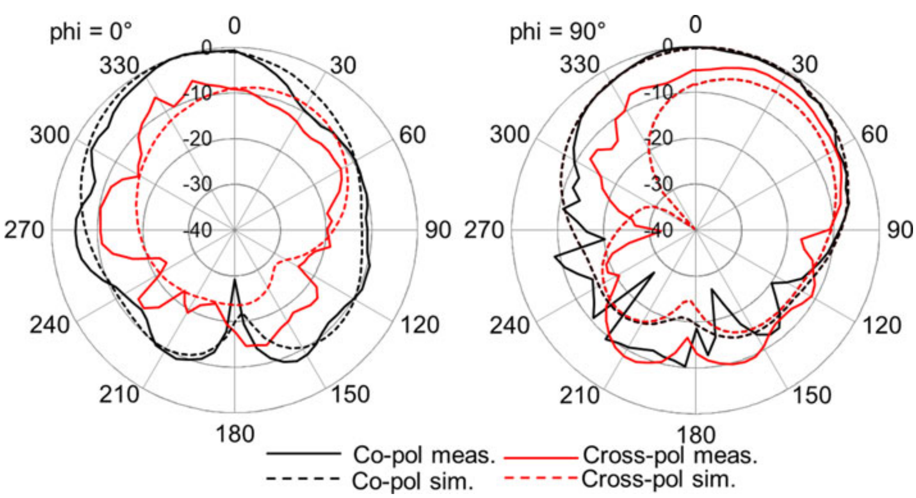

Fig. 13. Ant. II's radiation pattern at 4.65 GHz.

Table 2. Comparison of the proposed filtering antennas with previous studies

Configuration	Sharpest slope (dB/GHz)[a]	Gain (dBi)	Order
Microstrip and $\lambda/2$ resonator	66	6.7	Second
Microstrip and $\lambda/4$ resonator	95	6.8	Third
L and F inverted antenna using hairpin and stub resonator	125 and 80	1.02 and 0.11	Fourth and third
Microstrip and split-ring resonator	183/318/387 (no measurement validation)	5.5, 5.9 and 6.3	Third, fourth, and fifth
Microstrip and $\lambda/4$ resonator (Ant. I)	66	6.48	Second
Microstrip and $\lambda/4$ resonator (Ant. II)	118	6.37	Third

[a]The sharpest slope is calculated as G_{max}dB–20 dB/f_{max}–f_{20} dB GHz, where G_{max} is the maximum gain within the bandwidth, and f_{max} and f_{20} are, respectively, the frequency points regarding to the decrease from the maximum realized gain by 20 dB [21].

unidirectional pattern at $\phi = 0°$ and $\phi = 90°$, with main lobe directions both at $\theta = 0°$, and the cross-polarization discriminant at $\phi = 0°$ is around 12 dB in the broadside. The normalized simulation and measurement radiation pattern of Ant. II are shown in Fig. 13, where the filtering antenna shows a broadside radiation pattern with a cross-polarization discriminant around 10 dB. The shift between the simulation and measurement results for Ant. I and Ant II is due to the fabrication error.

Table 2 provides a comparison of our designs and the previous filtering antennas, and it shows that even if the reference [17] has the highest slope, it lacks the measurement validation. Reference [18] also has better selectivity than the proposed designs;

https://doi.org/10.1017/S1759078722001143 Published online by Cambridge University Press

however, it used a higher order and caused a very low gain value due to the higher loss in the transmission line.

Conclusion

In this paper, second- and third-order interdigital filtering antennas were designed, both of which have the same bandwidth and ripple, however the former has a wider rectangular radiator and lower Q_{rad} values compared to the latter. The simulation results showed that the third-order interdigital filtering antenna has improve the selectivity of the second-order from 66 to 118 dB/GHz, with a relatively flat gain over the operational bandwidth. Both antennas were fabricated and measured. The simulation and measurement results are consistent.

Acknowledgement. This work was partly supported by Hibah Internal UHAMKA under Contract No. 786/F.03.07/2022. The authors would like to thank the Telecommunication Laboratory of Electrical Engineering Department – Faculty of Engineering Universitas Indonesia for providing the measurement laboratory and CST software.

References

1. **Sen Wu Q, Zhang X and Zhu L** (2018) A wideband circularly polarized patch antenna with enhanced axial ratio bandwidth via co-design of feeding network. *IEEE Transactions on Antennas and Propagation* **66**, 4996–5003.
2. **Zhang X, Cao S, Chen J and Member S** (2021) Novel millimeter-wave bandwidth-controllable filtering antenna based on composite ESPPs-SIW structure. *IEEE Transactions on Antennas and Propagation* **69**, 7924–7929.
3. **Cahyasiwi DA, Zulkifli FY and Rahardjo ET** (2020) Switchable slant polarization filtering antenna using two inverted resonator structures for 5 G application. *IEEE Access* **8**, 224033–224043.
4. **Xie H, Wu B, Wang Y, Fan C, Chen J and Su T** (2021) Wideband SIW filtering antenna with controllable radiation nulls using dual-mode cavities. *IEEE Antennas and Wireless Propagation Letters* **20**, 1799–1803.
5. **Abdalla MA, El Atrash M, Aziz AAA and Abdelnaser MI** (2022) A compact dual-band D-CRLH-based antenna with self-isolation functionality. *International Journal of Microwave and Wireless Technologies* **14**, 616–625.
6. **Cahyasiwi DA and Rahardjo ET** (2018) Circular patch filtering antenna design based on hairpin band-pass filter, in *International Symposium on Antenna and Propagation*, pp. 263–264.
7. **Zhang X, Wang X, Tang S, Chen J, Member S and Yang Y** (2021) A wideband filtering dielectric patch antenna with reconfigurable bandwidth using dual-slot feeding scheme. *IEEE Access* **9**, 96345–96352.
8. **Liu H, Tian H, Liu L and Feng L** (2022) Co-design of wideband filtering dielectric resonator antenna with high gain. *IEEE Transactions on Circuits and Systems II: Express Briefs* **69**, 1064–1068.
9. **Al Yasir YIA, Alhamadani HA, Kadhim AS, Parchin NO, Saleh AL, Elfergani ITE, Rodriguez J and Abd-Alhameed R** (2020) Design of a wide-band microstrip filtering antenna with modified shaped slots and SIR structure. *Inventions* **5**, 1–10.
10. **Jiang ZH and Werner DH** (2015) A compact, wideband circularly polarized co-designed filtering antenna and its application for wearable devices with low SAR. *IEEE Transactions on Antennas and Propagation* **63**, 3808–3818.
11. **Wu Y and Mao C** (2019) Compact dual-polarized antenna for dual-band full-duplex base station applications. *IEEE Access* **7**, 72761–72769.
12. **Chin KL and Shyh JC** (2011) A compact filtering microstrip antenna with quasi-elliptic broadside antenna gain response. *IEEE Antennas and Wireless Propagation Letters* **10**, 381–384.
13. **Zhang XY, Duan W and Pan Y** (2015) High-gain filtering patch antenna without extra circuit. *IEEE Transactions on Antennas and Propagation* **63**, 5883–5888.
14. **Yin J-Y, Bai T-L, Deng J-Y, Ren J, Sun D, Zhang Y and Guo L-X** (2021) Wideband single-layer substrate integrated waveguide filtering antenna with U-shaped slots. *IEEE Antennas and Wireless Propagation Letters* **20**, 1726–1730.
15. **Atallah HA, Abdel-rahman AB, Yoshitomi K and Pokharel RK** (2018) Design of compact frequency agile filter-antenna using reconfigurable ring resonator bandpass filter for future cognitive radios. *International Journal of Microwave and Wireless Technologies* **10**, 487–496.
16. **Cahyasiwi A, Zulkifli FY and Rahardjo ET** (2019) Stacked interdigital filtering antenna with slant polarization, in *Conference on Antenna Measurement and Application*, pp. 6–9.
17. **Mansour G, Nugoolcharoenlap E, Lancaster MJ and Akkaraekthalin P** (2019) Comparison of different order filtering antennas, *RI2C 2019 – 2019 Res. Invent. Innov. Congr.*, pp. 2–6.
18. **Lin S, Chiou P and Chen Y** (2018) An accurate filtenna synthesis approach based on load-resistance flattening and techniques. *IEEE Access* **6**, 24568–24581.
19. **Matthaei GL, Young LEO and Jones EMT** (1985) *Microwave Filters, and Coupling Structures*. New Jersey, USA: Artech House.
20. **Hong J and Lancaster MJ** (2001) *Microstrip Filters for RF/Microwave*. New York, USA: A Wiley-Interscience Publication.
21. **Hu K, Tang M, Member S, Li M and Ziolkowski RW** (2018) Substrate integrated waveguide filtenna. *IEEE Antennas and Wireless* **17**, 1552–1556.

Dwi Astuti Cahyasiwi received her Bachelor, Magister, and Doctoral degrees in Electrical Engineering from the Universitas Indonesia in 1997, 2009, and 2022, respectively. She received Excellent Scholarship for Indonesia's Lecture (Beasiswa Unggulan Dosen Indonesia/ BUDI-LPDP) for her Doctoral degree. She is a member of IEEE Antenna and Propagation Society (AP-S) since 2021 and a reviewer of IEEE Access since 2020. Cahyasiwi was a recipient of the Best Student Paper Award at the 2019 IEEE Conference on Antenna Measurement and Applications (CAMA). Her research interests are integration design of antenna and filter, multiple-input multiple-output (MIMO), dual-polarized antenna systems, metasurface, polarization converter, and microwave circuits.

Emilia Roza received the Bachelor and Magister degrees in Electrical Engineering from the Universitas of Mercu Buana Indonesia in 1998 and 2015. Her research interests are antenna microstrip and filter.

Mohammad Mujirudin received the Bachelor degree in Electrical Engineering from the Universitas Hasanuddin in 1996, and Magister in Electric Engineering from Universitas Indonesia in 2003. He received Scholarship for Indonesia's Lecture (Beasiswa BPPS). His research interests are antenna, microstrip filter, and robotics control.

Nusriyati Mahmudah Nashuha received her Bachelor degree in Electrical Engineering from the Telkom University in 2011, and Magister in Electric Engineering from Universitas Indonesia in 2019. Her research interests are wireless communication, coding in multiple access, and antenna propagation.

https://doi.org/10.1017/S1759078722001143 Published online by Cambridge University Press

Fitri Yuli Zulkifli received her Bachelor and Ph.D. degrees in Electrical Engineering from Universitas Indonesia (UI) in 1997 and 2009, while M.Sc. degree from Karlsruhe Institute of Technology, Germany in 2002. Her research interests are antenna, propagation, microwave, and in the field of telecommunication. She joined the Antenna Propagation and Microwave Research Group (AMRG) UI since 1997 and has become lecturer in Electrical Engineering Department UI since 1998. Prof. Yuli has published more than 200 papers in journals/conference proceedings and received more than 40 research grants. She now leads "Laboratory Prof. Fitri Yuli Zulkifli" and also the head of professional engineering study program in UI. From 2011 to 2012 she became the joint chapter chair of MTT/AP Indonesia. In 2017–2018, she was the IEEE Indonesia Section Chair and from 2019 to 2022, she has been serving as a committee member for R10 Conference and Technical Seminar and Conference Quality Management.

Eko Tjipto Rahardjo received B. Eng. degree from Universitas Indonesia, Indonesia, in 1981, the M.S. degree from the University of Hawaii, USA, in 1987, and the Ph.D. degree from Saitama University, Japan, in 1996, all in Electrical Engineering. He has been the Director of Antenna Propagation and Microwave Research Group (AMRG), Universitas Indonesia. His research interests include antenna engineering, wave propagation, microwave circuits and communication systems, and telecommunication system regulations. He has published and presented more than 200 research articles both in national and international journals and symposiums. Prof. Rahardjo is a member of the IEEE Antenna and Propagation Society (AP-S) and the IEEE Microwave Theory and Technique Society (MTTS) and has been actively participating in the National and International Committee as the International Advisory Board, Steering Committee, or General Chair in the International Symposium on Antenna and Propagation (ISAP), Asia Pacific Microwaves Conference (APMC), and IEEE Conference on Antenna Measurement and Applications (CAMA).